Title
A STUDY OF THE ODD-A RHENIUM ISOTOPES: 179Re AND 177Re

Authors
Leigh, J.R.
Newton, J.O.
Ellis, L.A.
et al.

Publication Date
1971-06-01

Submitted to Nuclear Physics

UCRL-20494
Preprint

A STUDY OF THE ODD—A RHENIUM ISOTOPES: ^{179}Re AND ^{177}Re

J. R. Leigh, J. O. Newton, L. A. Ellis,
M. C. Evans, and M. J. Emmott

June 1971

AEC Contract No. W-7405-eng-48

UCRL-20494

DISCLAIMER

UCRL-20494

A STUDY OF THE ODD-A RHENIUM ISOTOPES: ^{179}Re AND ^{177}Re *

J. R. Leigh†

Lawrence Radiation Laboratory
University of California
Berkeley, California 94720

J. O. Newton†, L. A. Ellis, M. C. Evans, and M. J. Emmott

Department of Physics
The University
Manchester, England

June 1971

Abstract: Gamma-rays following $^{172}Yb(^{11}B,4n)^{179}Re$ and $^{169}Tm(^{12}C,4n)^{177}Re$ reactions have been studied with Ge(Li) detectors. Rotational bands based on the $1/2^-[541]$, $5/2^+[402]$ and $9/2^-[514]$ states have been populated. A pronounced variation in the energies of the quasi-particle levels is apparent although the quadrupole deformation of the isotopes below mass 183 is expected to be fairly constant. It is suggested that the variation is related to the changing hexadecapole moments of these nuclei.

NUCLEAR REACTIONS $^{172}Yb(^{11}B,4n)$ E = 52-60 MeV
$^{169}Tm(^{12}C,4n)$ E = 62-76 MeV
measured $\sigma(E; E_\gamma, 0_\gamma)$ $\gamma\gamma$-coin., ^{177}Re, ^{179}Re deduced levels J, π.

* Work performed in part under the auspices of the U. S. Atomic Energy Commission.

† Present address: Dept. of Nucl. Phys., Research School of Physical Sciences, The Australian National University, Canberra.

1. Introduction

The odd mass nuclei $^{181-187}$Re are located near to the upper end of the rare-earth deformed region. They have in recent years been studied in a variety of ways including radioactive decay studies[1-7], inelastic scattering[8], resonance fluorescence[9,10], particle, xn reactions[11-15] and single-nucleon transfer reactions[16]. Heavy-ion, xn (HI,xn) reactions afford a method of extending the range of the neutron-deficient rheniums which can be studied, the limit being set by competition from charged particle evaporation[17,18]. It is of considerable interest to study a large range of odd-mass nuclei having one particle number unchanged. In this way the effect on the nuclear states of changing only one particle number can be investigated without the complications and uncertainties arising from changing the other. To date there are rather few cases where level schemes are known in any detail for such ranges of even as many as four nuclei and most of these have a closed shell for the unchanged particle group.

We have investigated the level schemes of $^{175-181}$Re, thus extending the number studied to seven. To do this we used the methods of in-beam HI,xnγ spectroscopy and also studied the electron-capture decay of the appropriate neutron deficient osmium isotopes produced in HI,xn reactions. In this paper we report on the level schemes of ^{177}Re and ^{179}Re studied by the former method.

2. Experimental Method

The HILACS at Manchester University and Berkeley have both been utilized in this work. The Manchester machine, with a duty cycle of 2.5%, was used to accelerate ^{11}B and ^{12}C ions for measurement of excitation functions of the $^{172}Yb(^{11}B,4n\gamma)^{179}Re$ and $^{169}Tm(^{12}C,4n\gamma)^{177}Re$ reactions. The de-excitation gamma-rays were recorded both in-beam and out-of-beam, using Ge(Li) detectors of active volumes 4 cc and 25 cc with resolutions (FWHM at ^{60}Co) of 3.0 keV and 2.2 keV, respectively. The targets were self-supporting metallic foils of approximately 3 mg/cm^2, obtained by rolling between tantalum sheets. The ^{172}Yb was enriched to 98% and was reduced from the oxide form by the method of Westgaard and Bjornholm[19]. The Ge(Li) detectors were located at 90° to the beam direction. The beam was stopped about 3 meters from the target in a Faraday cup, which was surrounded with concrete and lead. Background radiation arising from sources other than the target was negligible.

The Berkeley HILAC, with a 20% duty cycle, has been used to provide ^{12}C beams at 72 MeV and ^{11}B ions at 53 MeV. Gamma-gamma coincidence measurements were performed with two Ge(Li) detectors placed opposite each other and at 90° to the beam direction. The beam was stopped in a Faraday cup and again background from sources other than the target was neglibible. A multi-dimensional program was used in conjunction with a PDP-7 computer system to record coincidence events. A fast-slow coincidence arrangement was used incorporating a time-to-amplitude converter with a logarithmic pulse height compensating system[20]. Resolving times of about 15 ns were typical.

Angular distributions of the de-exciting γ-rays in ^{177}Re were measured, at Berkeley, with a movable Ge(Li) detector and a fixed detector as a monitor.

The very intense Coulomb excitation gamma-rays from the target were used for normalization purposes. The target chamber was a vertical aluminium cylinder, coated on the inside with lead foil, thick enough to stop the incident beam. Measurements could therefore be made at 0° to the beam direction. The full details of the method are described in Ref. [21]). The 5 msec beam pulse of the Berkeley HILAC could be chopped using an electrostatic deflector system. In this way continuously variable pulse widths (as short as 0.25 μsecs) and repeat intervals (minimum 2.5 μsecs) can be obtained. This facility has been used to search for isomers in the two isotopes studied here.

The energy calibrations and relative efficiency curves for the Ge(Li) detectors were obtained using ^{177m}Lu and I.A.E.A. standard gamma-ray sources.

3. Results

3.1. GAMMA-RAY SPECTRA AND EXCITATION FUNCTIONS

In-beam gamma-ray spectra, obtained with 53 MeV ^{11}B ions and 72 MeV ^{12}C ions incident on ^{172}Yb and ^{169}Tm are shown in fig. 1. The energies and relative intensities of the observed transitions in ^{179}Re and ^{177}Re are shown in Tables 1 and 2. The relative intensities have been corrected for detector efficiency, attenuation in absorbers and conversion electron emission. For the latter we used theoretical conversion coefficients[22]), assuming the assignments given in Tables 1 and 2 to be correct.

Excitation function data can be a useful aid in deducing the angular momenta of populated states[12]). However, due partly to the greater effective target thickness with the heavier ions, the effects observed in this work are not as pronounced as those of Ref. [12]). Nevertheless the excitation functions can be used to support the proposed schemes, as can be seen from some results shown in figs. 2 and 3.

Two isomeric transitions were observed in the out-of-beam spectra. A 65.3 γ-ray with $\tau_{1/2} = 95 \pm 25$ μs was attributed to ^{179}Re and an 84.7 keV γ-ray with $\tau_{1/2} = 50 \pm 10$ μs was assigned to ^{177}Re. Both assignments were made on the basis of the excitation functions.

3.2. COINCIDENCE MEASUREMENTS AND LEVEL SCHEMES

Typical spectra taken in coincidence with the 185 keV and 214 keV γ-rays of ^{177}Re and with the 169 keV and 218 keV γ-rays of ^{179}Re are shown in fig. 4. In both nuclei three independent sets of coincident gamma rays are observed. The relative level positions in each set were determined by the relative intensities of the gamma rays and also by cross-over gamma-rays which were seen in the singles spectra and in a few cases in the coincidence spectra also.

The level schemes deduced in this way for both nuclides are shown in figs. 5 and 6. Sets I and II have characteristics typical of rotational bands. The energies of the levels are given approximately by the $J(J + 1)$ rule and the excitation function data indicates that the angular momentum of the states increases with excitation energy. Set III does not appear to be of such a simple nature as no cross-over transitions are seen, nor do the energies even approximately obey a simple $J(J + 1)$ rule. However, the excitation functions do indicate that the angular momentum of the levels increases with excitation energy.

If an hypothesis of three rotational bands were correct then at least two transitions between them must exist in each nucleus. These transitions would have to have the same intensity as the total intensities populating the bands from which they decay. They would, therefore, be expected to have only slightly greater intensity than those of the lowest transitions in the bands, since in HI,xn reactions the direct population of the lowest state of a rotational band is normally much less than that from the remainder of the band. The only ones which we observe which could fit into this category are the isomeric 65.3 keV and 84.7 keV γ-rays in ^{179}Re and ^{177}Re, respectively. We have no direct measure of the multipolarity of these transitions. However, if we assume that their intensities cannot greatly exceed those of the strongest rotational transitions we can deduce on the basis of theoretical conversion coefficients, that the 84.7 keV transition must be E1 and the 65.3 keV transition E1 or M1. For reasons which will be given later we prefer the E1 assignment for the 65.3 keV transition, and this and the 84.7 keV transition are placed as shown in figs. 5 and 6. However, we must emphasize that the arguments advanced in favour of these assignments are entirely based on plausibility considerations and accordingly they may be in error.

3.3. ANGULAR DISTRIBUTION MEASUREMENTS

States formed in HI,xn reactions have their angular momentum vectors strongly and systematically aligned in the plane perpendicular to the beam direction. This alignment gives rise to strongly anisotropic γ-ray angular distributions and therefore provides a useful spectroscopic tool[23,24]. The angular distributions are of the form

$$W(\theta) = 1 + \sum_{k_{even}} A_p \, P_k(\cos\theta) \ .$$

The coefficients A_k are related to the coefficients $A_k(1/2)$, appropriate for the decay of a given level of spin J in the M = 1/2 substate, by the relation

$$A_k = G_k(J) \, A_k(1/2) \ .$$

The coefficients $G_k(J)$ may be estimated from systematic data from other HI,xn reactions where the level spins and transition multipolarities are known. Plots of the $G_2(J)$ and $G_4(J)$ so derived for doubly-even nuclei are given in Ref. [25]). In cases where a level decays by two transitions, one of which is known to be a pure multipole, the $G_k(J)$ may be determined directly. A full discussion of the procedures used to interpret the angular distributions is given in Refs. [12,24]).

The experimental values of A_2 and A_4 for transitions in ^{177}Re deduced with a least squares fitting program are listed in Table 2. The coefficients tend to fall mainly into two classes, one with very small values of A_2 and A_4 and the other having values of A_2 of about +0.3 and negative A_4. Similar behaviour was seen in the ^{181}Ta(^{4}He,2n)^{183}Re experiment and was shown to be expected[12]). The

angular distributions with small coefficients can arise from the M1/E2 transitions between adjacent levels within rotational bands; the coefficients are small when there is a few per cent admixture of E2 and when the amplitude of the mixing ratio δ is positive, as expected for odd-proton nuclei. The other class of coefficients can arise from the stretched E2 cross-over transitions within the bands. This interpretation is in full accordance with that which would be expected from the proposed rotational level schemes for bands I and II of fig. 6. The angular distributions from the transitions in band III, where it was possible to measure them, are consistent with their being of stretched E2 character. The very great similarity between the level schemes of ^{179}Re and ^{177}Re (figs. 5 and 6) has been used in assigning the multipolarities of the transitions in ^{179}Re (see Table 1).

In order to determine the M1/E2 mixing ratios from the angular distribution measurements for bands I and II it is necessary to estimate the alignment coefficients $G_k(J)$. This was done by comparing the observed A_2 values for the proposed stretched E2 transitions with those calculated for decay from states completely aligned in the M = 1/2 state[26]). The degree of alignment obtained is consistent with that observed in other reactions induced by ions of similar mass. The average value of A_2 for the stretched E2 transitions, in ^{177}Re and ^{172}Hf is 0.33 ± 0.03 and 0.35 ± 0.02, where the ^{172}Hf was produced by the reaction ^{165}Ho(^{11}B,4n)^{172}Hf. The values for δ which we obtained are given in Table 3 and compared with those estimated from the rigid rotor model. The agreement is generally within the experimental errors.

4. Discussion

4.1. BAND ASSIGNMENTS

There is very little previous information on the nuclides studied in this work. Only one inter-band transition was observed in each nucleus and the assignments of these were very tentative. Thus in order to assign spins and parities to the observed states, it is necessary to rely largely on the systematics of nuclei in this region. However the use of systematics is only likely to be reliable if properties such as deformation remain fairly constant over the mass range of interest. In fig. 7 the energies of the first excited states of the neighbouring doubly-even nuclei are plotted against neutron number N. The energies vary very little over the range N = 100-108, though outside this region they increase fairly rapidly. This suggests that the deformation is fairly constant within this range and falls off rapidly on either side of it. Such behaviour is not unexpected, since N = 104 corresponds to the N = 82-126 shell being half full, where on a naive picture, the greatest deformation would be obtained for a given value of Z. Therefore it seems that systematics may well be a good guide in making assignments to ^{179}Re and ^{177}Re, with N = 104 and 102, respectively.

In the odd-mass nuclei $^{181-187}$Re the ground state can be assigned fairly definitely to the $5/2^+[402]$ Nilsson orbital. The $9/2^-[514]$ state is seen to be low lying in all of these nuclei[1,13-16]. The $1/2^-[514]$ state has also been identified and is relatively low lying in ^{183}Re and ^{181}Re. The rotational band based on this state has a large decoupling parameter and splits up in effect into two bands, whose successive states differ in angular momentum by two units. The transitions within these sub-bands are therefore pure stretched E2

transitions. Although states corresponding to other Nilsson orbitals have also been observed in some of these nuclei, only the rotational bands based on $5/2^+[402]$, $9/2^-[514]$ and $1/2^-[541]$ orbitals were seen to be significantly populated in HI,xn reactions[12-14]). The reason is that they provide in each case the states of highest angular momentum at lowest excitation energy.

The energy systematics of a number of the observed Nilsson base states for the odd rhenium nuclei are shown in fig. 8a. The excitation energies of the $9/2^-[514]$ and the $1/2^+[411]$ states rise with decreasing mass number to a maximum at A = 183 and then decrease. On the other hand the energy of the $1/2^-[541]$ state decreases continuously below A = 187 [16]). A possible reason for this behaviour of the levels is given later.

If it were legitimate to extrapolate the trends of the levels shown in fig. 8a to ^{179}Re and ^{177}Re we would expect that the $9/2^-[514]$ and $1/2^-[541]$ levels would become very low lying. In fact the ground state in these nuclei might even be the 9/2 $9/2^-[514]$ state or the lowest member of the $1/2^-[541]$ rotational band which is most probably the $5/2^-$ state[12,27]). Although the relative positions of the levels are markedly changing with N, it would seem reasonable to expect that the gross properties of the rotational bands, such as moment of inertia, would stay approximately constant because they do so in the neighbouring doubly-even nuclei. On this general basis we assign bands I, II and I to the $9/2^-[514]$, $5/2^+[402]$ and $1/2^-[541]$ Nilsson orbitals. The energies of the 11/2 $9/2^- \rightarrow$ 9/2 $9/2^-$, 7/2 $5/2^+ \rightarrow$ 5/2 $5/2^+$ and 13/2 $1/2^- \rightarrow$ 9/2 $1/2^-$ transitions of these bands are plotted in fig. 7 as a function of N. They are to be compared with the energies of the first excited states of the neighbouring doubly-even nuclei, also given in fig. 7. The correlation between the

general trend for the doubly-even nuclei and for the $5/2^+$ and $9/2^-$ bands is very striking, supporting strongly the above assignments. There is a less good correlation with the $1/2^-$ band, in that the excitation energies of the $13/2 \rightarrow 9/2$ transitions rise more rapidly with decreasing N than those for the 2^+ states; nevertheless the rise is smooth favouring the assignment. The reason for the different behaviour of the $1/2^-$ band will be explained later. It arises from the fact that the band is strongly Coriolis mixed and that the degree of mixing decreases with decreasing N.

We now consider the relative excitation energies of the three bands and the arguments in favour of our assignments of the isomeric 65.3 keV and 84.7 keV transitions in ^{179}Re and ^{177}Re, respectively (see figs. 5 and 6). We have already remarked that extrapolation of the systematics for $^{181\text{-}187}$Re suggests that the three bands will lie close together. This conclusion is further supported by the data on the relative population of the bands. This is illustrated in fig. 8b, where we plot the transition intensity of the lowest state of each band, inter-band transitions being subtracted, expressed as a percentage of the sum of these intensities for the three bands. As a rough guide one would expect that, if the reaction were statistical in nature, the population would be about the same for each band when the spin 9/2 states of each band had the same excitation energy. The higher the excitation energy of the 9/2 state the lower would be its population. A comparison of figs. 8a and 8b shows that there is a strong correlation between the variation of level position and band population, though there is not exactly equal population when 9/2 states are at the same energy as in ^{181}Re. From fig. 8b we expect that the $9/2^-$ and $1/2^-$ bands have both dropped further in excitation energy in

^{179}Re compared with ^{181}Re. It is even possible that the $9/2^-[514]$ state may have become the ground state. The $1/2^-[541]$ band is most strongly populated in ^{177}Re and it is possible that the lowest state of this band, probably the $5/2^-$ rotational state, is at or near the ground state.

In order to discuss our assignments for the two isomeric transitions we have to consider the possible transitions between the bands. We shall assume that these occur only from the lowest states in the bands as they do in the other rhenium nuclei. The prominent E1 transition between the 9/2 $9/2^-$ state and the 7/2 $5/2^+$ state seen in $^{181\text{-}187}$Re clearly does not occur in ^{177,179}Re. This is shown by the intensity of the 7/2 $5/2^+ \rightarrow$ 5/2 $5/2^+$ transition being nearly equal to that feeding the $7/2^+$ state from within the $5/2^+$ band. The 9/2 $9/2^-$ state must therefore be extremely close to or below the 7/2 $5/2^+$ state in these nuclei. The transition between these two bands must therefore be of M2 multipolarity between the 9/2 $9/2^-$ and 5/2 $5/2^+$ states. It would be expected to have a half-life of order 1 - 10 μs if the matrix element had a value around that for ^{183}Re. Its γ-ray intensity would moreover be expected to be low since the conversion coefficient is about 10 even for an energy as high as 150 keV. It is therefore unlikely that this transition would be observed.

Intensity considerations similarly rule out the occurrence in ^{177,179}Re of the E1 transition, seen in ^{181,183}Re, between the 5/2 $1/2^-$ state and the 7/2 $5/2^+$ state. An E1 transition could, however, occur between the 5/2 $1/2^-$ state and the 5/2 $5/2^+$ state. In ^{183}Re this transition was not observed and is more than 20 times weaker than the 5/2 $1/2^- \rightarrow$ 7/2 $5/2^+$ transition. Transitions between the $9/2^-$ and $1/2^-$ bands can be the E2 transition between the 9/2 $9/2^-$

and the 5/2 1/2$^-$ states and, if the 9/2 9/2$^-$ state is above the 9/2 1/2$^-$ state, the M1 transition between these two states. If both could occur it is likely that the M1 transition would be most favoured, since it could take place between the 7/2$^-$[514] component of the Coriolis mixed 9/2 1/2$^-$ state and the 9/2 9/2$^-$[514] state. According to Tables 5 and 6, which give the calculated amplitude for the 7/2$^-$[514] component, we would expect a hindrance factor of about 10^5 for this transition. No E2 transition allowed by the asymptotic selection rules occurs between the states which are likely to be strongly mixed into the 9/2$^-$ or 1/2$^-$ bands.

If we accept the assumption that the 65.3 keV and 84.7 keV γ-rays do arise from transitions between the lowest states of the bands, we can on the basis of the above conclude that the E1 84.7 keV transition must occur between the 5/2 5/2$^+$ and 5/2 1/2$^-$ states. Its intensity is consistent with it arising from the 5/2 5/2$^+$ state and not from the 5/2 1/2$^-$ state. This places the latter below the former in ^{177}Re, which is in accordance with expectations from fig. 8b. If the 65.3 keV transition were M1 it would place the 9/2 9/2$^-$ state 64.3 keV above the 9/2 1/2$^-$ state in ^{179}Re. The band populations shown in fig. 8b would however suggest that in this nucleus the 9/2 9/2$^-$ state was the lower of the two. On the other hand if the 65.3 keV transition were E1, its intensity would be in accordance with it arising from the decay of the 5/2 1/2$^-$ state to the 5/2 5/2$^+$ state. This would be in reasonable agreement with expectations from fig. 8b.

We therefore very tentatively assign the 84.7 keV transition in ^{177}Re to the decay of the 5/2 5/2$^+$ state to the 5/2 1/2$^-$ state and the 65.3 keV transition in ^{179}Re to the decay of the 5/2 1/2$^-$ state to the 5/2 5/2$^+$ state.

If these assignments are correct, both of the E1 transitions are highly hindered. The hindrance factors relative to the single-particle values are $(2.2 \pm 0.6) \cdot 10^8$ and $(3.4 \pm 0.7) \cdot 10^8$ for the 65.3 keV and 84.7 keV transition, respectively.

4.2. EXCITATION ENERGIES OF BAND HEADS

Whilst the moments of inertia both of the doubly-even and of the odd-mass nuclei change rather little over the region of N = 100 to 108 (fig. 7), the relative energies of the quasi-particle levels change very markedly. It seems unlikely that these energy variations could be related to changes in the quadrupole deformation as these would almost certainly be reflected in changes in the observed moments of inertia.

The equilibrium calculations of Nilsson et al.[28], based on the Stutinsky method, suggest that for Z = 75 the quadrupole deformation parameter ϵ decreases fairly rapidly as N increases from 108 and remains fairly constant in the region from N = 108 to 100. On the other hand the hexadecapole deformation parameter, ϵ_4, has a fairly constant value of +0.055 for $N \geq 108$ but decreases rapidly when N falls below 108, reaching a value of about +0.02 at N = 100. In fig. 9 we show the energies of a number of single-particle levels, as a function of ϵ_4, for a fixed value of $\epsilon = 0.25$. The curves are deduced by interpolation and extrapolation from the calculations of Nilsson et al.[28]. For a number of reasons one cannot expect an exact correspondence between the relative positions of these levels and of the experimental ones. However, it is quite clear from fig. 9 that, if ϵ_4 has a value of about +0.05 for ^{183}Re and decreases with decreasing N, we shall get just the type of behaviour which actually occurs in the odd rhenium nuclei

(fig. 8). The $9/2^-[514]$ hole state becomes the ground state at around $\epsilon_4 = +0.01$ and the $1/2^-[541]$ state becomes the ground state at $\epsilon_4 = -0.03$. The $1/2^-[541]$ state appears to be placed too high above the other two in fig. 9; if it were lower it would become the ground state nearer to $\epsilon_4 = 0$. Since this state originates from the $h_{9/2}$ level in the next higher shell a small error in its position would not be at all surprising. Additional support for this interpretation comes from the fact, shown later, that the Coriolis mixing in the $1/2^-[541]$ band decreases as N decreases. The nearest level which would be expected to be strongly involved in the mixing is the $3/2^-[532]$. From fig. 9 it is apparent that the spacing between the two levels increases with decreasing ϵ_4 and hence decreasing N. This would qualitatively give just the observed effect.

The behaviour of the levels shown in fig. 8a as N increases from 108 can be explained on the basis of decreasing ϵ, and constant ϵ_4. This will cause the $1/2^+[411]$, $9/2^-[514]$ states to come nearer to the $5/2^+[402]$ ground state and the $1/2^-[541]$ to move further away. This explanation of the level behaviour is as satisfactory as can be expected in view of the limitations of the theory and may well be the correct one. If so it suggests that studies of level positions for an isotopic series may give a useful indication of changes in the hexadecapole deformation parameter.

4.3. CORIOLIS MIXING IN THE $1/2^-[541]$ ROTATIONAL BAND

Rotational bands built on the $1/2^-[541]$ state have been observed in several odd-Z nuclei in this region. In all cases the effective moment of inertia and decoupling parameter appear much larger than expected from the Nilsson model and the level spacings cannot be fitted with the simple

rotational formula. In the case of ^{183}Re, Newton[12]) showed qualitatively that this could be explained by Coriolis mixing of all states in the $h_{9/2}$ orbit. Subsequent work on other deformed nuclides[27,29]) has produced similar cases where the levels involved arise from a shell model orbit of high spin. Detailed Coriolis mixing calculations have indeed given good fits to the observed energy level spacings using values for the rotational constant and decoupling parameter close to those predicted by the Nilsson model[30]).

A Coriolis coupling calculation has been performed to fit the transitions observed in this work. All states arising from the $h_{9/2}$ shell have been considered and couplings with other states neglected. The number of parameters which can be varied in a Coriolis calculation is large. In our case, these are the four relative energies of the quasi-particle states arising from the $h_{9/2}$ orbital, the four Coriolis matrix elements between them, the decoupling parameter $\underline{a}$ and the parameters A, B, etc., which occur in the expansion of the unperturbed rotational energies as a power series in $I(I + 1)$. In attempting to fit the data it seems more physically reasonable to attempt to fix some of these parameters on the basis of theory or systematics rather than to allow all of them to vary freely. If we are able to do this and also succeed in getting reasonable values for the variable parameters we may have some confidence that the general basis of the calculation is correct.

In this calculation we have made the following assumptions:

1) That the quasi-particle energies are given by

$$E_{qp}^{K} = \sqrt{(\varepsilon_K - \lambda)^2 + \Delta^2} - \Delta$$

where the ε_K's are the Nilsson single-particle energies, λ is the energy of the Fermi-surface and 2Δ the pairing energy, which we have taken to be 2 MeV.

2) That the unperturbed rotational energies of the bands are given by

$$E_K^I = E_K^0 + A[I(I+1) + (-1)^{I+\frac{1}{2}}(I+\tfrac{1}{2})\, a\delta_{K\frac{1}{2}}]$$

$$+ B[I(I+1) + (-1)^{I+\frac{1}{2}}(I+\tfrac{1}{2})\, a\delta_{K\frac{1}{2}}]^2$$

where E_K^0 is chosen such that $E_K^K = 0$.

3) That the Coriolis coupling matrix elements are given by

$$H^I_{K,K+1} = \sqrt{I(I+1) - K(K+1)}\ \langle K|j_-|K+1\rangle \ .$$

The quantities $\langle K|j_-|K+1\rangle$ can be evaluated from the Nilsson wave-functions and these values have been assumed, except for the case of $\langle 1/2|j_-|3/2\rangle$ which has been allowed to vary. This has been done because a reduction below the Nilsson value is expected when the $K = 1/2^-$ state is near to the Fermi-surface.

4) That the quadrupole deformation parameter $\delta = 0.25$. This value is close to those of the doubly-even neighbours[31]) and it was verified that the results of the calculation were not very sensitive to small changes in δ.

The resulting matrix has been diagonalized using the program BETABLE, written by T. Clements, which allows any of the parameters A, B, a, $\langle K|j_-|K+1\rangle$ or E^K_{qp} to be varied to give the best fit to the experimentally observed energy levels.

The sequence of E2 transitions observed in our experiments locates only the $I = 2n + 1/2$ ($n = 1, 2, \ldots$) members of the band and these alone may be satisfactorily fitted with widely differing combinations of $\underline{a}$ and A. The predicted positions of the $I = 2n - 1/2$ members are however very sensitive to changes in these parameters. We therefore chose to fit, as a starting point, the levels of ^{181}Re, since in this case the energies of the $1/2^-$ and $3/2^-$ members of the band, and of the $3/2^-[532]$ band head are also known[2]). The positions of the energy levels were then fitted with A, B, $\underline{a}$ and $\langle 1/2|j-|3/2\rangle$ as parameters. The position of the Fermi-surface was chosen to give the appropriate energy separation of the $1/2^-[541]$ and $3/2^-[532]$ band heads. The best fit was obtained with the full Nilsson value for the Coriolis matrix element and with a value for $\underline{a}$ close to the Nilsson value of 3.9 (see Table 7). The values obtained for the other parameters are shown in Table 4.

The energies of the $1/2^-$ and $3/2^-$ band heads are not available for ^{179,177}Re. However, the quadrupole deformation for these nuclei is not expected to change significantly to that for ^{181}Re (see fig. 7), so that we felt it reasonable to use the same values for A and $\underline{a}$ in these cases as for the case of ^{181}Re. When we used the full Nilsson value for $\langle 1/2|j-|3/2\rangle$ and only allowed variation of B and the unknown $1/2^-[541] - 3/2^-[532]$ energy separation we obtained excellent fits (see Tables 5 and 6) with the parameters shown in Table 4. The increasing $1/2^-[541] - 3/2^-[532]$ energy spacings with decreasing mass, indicated by these fits, is consistent with the expected decrease in hexadecapole deformation with decreasing mass (see fig. 9). However, the magnitude of the change is larger than expected.

Fits of similar quality can be obtained if the band-head spacing increases more slowly with decreasing mass and at the same time the Coriolis

matrix element linking them is decreased. Such an effect might be expected from pairing considerations since, both experimentally and theoretically, on the basis of decreasing ε_4 with decreasing mass, the $1/2^-[541]$ state is approaching the Fermi-surface as the mass decreases.

Although it would be unreasonable to expect perfect fits to the data from such calculations, those obtained are very good and do result in very reasonable values for the parameters varied. Moreover the calculations are in qualitative accord with the hypothesis that ε_4 is decreasing with decreasing mass. It can therefore be concluded that they support the general proposals of this paper.

Acknowledgements

We would like to express our gratitude to Drs. R. M. Diamond and F. S. Stephens for permitting the use of their apparatus and their machine-time for some of these studies. One of us (JRL) is deeply grateful to them for their hospitality and many enlightening discussions during his stay at Berkeley. Thanks are also due to Mr. T. L. Morgan who provided all the targets.

References

1) C. M. Lederer, J. M. Hollander, and I. Perlman, Table of Isotopes, 6th ed., J. Wiley and Sons, Inc., New York (1967).

2) B. Harmatz and T. H. Handley, Nucl. Phys. A121 (1968) 481.

3) A. E. Ellis, J. O. Newton, M. Evans, and J. R. Leigh, to be published.

4) A. W. Herman, E. A. Heighway, and J. D. MacArthur, Can. J. Phys. 48 (1970) 1040.

5) A. I. Akhmadzharov et al., Ak Nauk S.S.R. 34 (1970) 655.

6) K. J. Hofstetter and P. J. Daly, Phys. Rev. 152 (1966) 152.

7) P. F. A. Goudsmit, J. Konijn, and F. W. N. de Boer, International Conference on Nuclear Structure, Tokyo, Japan (1967).

8) K. M. Bisgaard and E. Veje, Nucl. Phys. A103 (1967) 545.

9) F. R. Metzger, Phys. Rev. 157 (1967) 1060.

10) H. Langhoff, Phys. Rev. 159 (1967) 1033.

11) M. J. Emmott, J. R. Leigh, J. O. Newton, and D. Ward, Phys. Letters 20 (1966) 56; ibid. 22 (1966) 719.

12) J. O. Newton, Nucl. Phys. A108 (1968) 353.

13) S. A. Hjorth, H. Ryde, and B. Skarberg, Arkiv Fysik 38 (1968) 537.

14) M. Evans, A. E. Ellis, J. R. Leigh, and J. O. Newton, Phys. Letters 34B (1971) 609.

15) T. W. Conlon, Nucl. Phys. A136 (1969) 70.

16) M. T. Lu and W. P. Alford, Phys. Rev. C 3 (1971) 1243.

17) J. O. Newton, Progress in Nuclear Physics 11 (1969) 53 (Pergamon Press).

18) F. S. Stephens, J. R. Leigh, and R. M. Diamond, submitted to Nucl. Phys.

19) L. Westgaard and S. Bjornholm, Nucl. Inst. and Methods 42 (1966) 77.

20) J. M. Jaklevic, F. M. Bernthal, J. O. Radeloff, and D. A. Landis, Nucl. Inst. and Methods 69 (1969) 109.

21) J. O. Newton, F. S. Stephens, R. M. Diamond, K. Kotojima, and E. Matthias, Nucl. Phys. A95 (1967) 357.

22) R. S. Hager and E. C. Seltzer, Nucl. Data A4 (1968).

23) H. Ejiri, M. Ishihara, M. Sakai, K. Katori, and T. Inamura, Phys. Letters 18 (1965) 34.

24) R. M. Diamond, E. Matthias, J. O. Newton, and F. S. Stephens, Phys. Rev. Letters 16 (1966) 1205.

25) J. O. Newton, S. D. Cirilov, F. S. Stephens, and R. M. Diamond, Nucl. Phys. A148 (1970) 593.

26) T. Yamazaki, Nucl. Data A3 (1967).

27) S. A. Hjorth and H. Ryde, Phys. Letters, 31B (1970) 201.

28) S. G. Nilsson et al., Nucl. Phys. A131 (1969) 1.

29) S. A. Hjorth, H. Ryde, K. A. Hagenann, G. Løvhøiden, and J. C. Waddington, Nucl. Phys. A144 (1970) 513.

30) S. G. Nilsson, Dan. Mat. Fys. Medd. 29 No. 16 (1955); B. R. Mottelson and S. G. Nilsson, Mat. Fys. Skr. Dan. Vid. Selsk 1 No. 8 (1959).

31) P. H. Stelson and L. Grodzins, Nucl. Data A1 (1965).

Table 1. Gamma-ray transitions observed in the $^{172}Yb(^{11}B,4n\gamma)^{179}Re$ reaction

E_γ	Relative γ Intensity	Assigned Multi-polarity	Relative Transition Intensity	Transition Assignment
65.3±0.3	78±25	E1	98±30	$5/2\ 1/2^- \rightarrow 5/2\ 5/2^+$
123.8±0.1	41±5	M1	159±19	$7/2\ 5/2^+ \rightarrow 5/2\ 5/2^+$
155.6±0.1	43±5	M1	108±13	$9/2\ 5/2^+ \rightarrow 7/2\ 5/2^+$
165.5±0.1	100±4	M1	227±9	$11/2\ 9/2^- \rightarrow 9/2\ 9/2^-$
168.7±0.1	75±4	E2	116±6	$13/2\ 1/2^- \rightarrow 9/2\ 1/2^-$
186.1±0.2	31±3	M1	58±6	$11/2\ 5/2^+ \rightarrow 9/2\ 5/2^+$
194.3±0.1	106±6	M1	191±11	$13/2\ 9/2^- \rightarrow 11/2\ 9/2^-$
211.1±0.3	28±8	M1	46±13	$13/2\ 5/2^+ \rightarrow 11/2\ 5/2^+$
217.8±0.1	69±7	M1	110±11	$15/2\ 9/2^- \rightarrow 13/2\ 9/2^-$
237.1±0.3	25±3	M1	36±4	$15/2\ 5/2^+ \rightarrow 13/2\ 5/2^+$
241.4±0.2	47±5	M1	67±7	$17/2\ 9/2^- \rightarrow 15/2\ 9/2^-$
252.7±0.3	12±3	M1	17±4	$17/2\ 5/2^+ \rightarrow 15/2\ 5/2^+$
257.8±0.2	22±2	M1	30±3	$19/2\ 9/2^- \rightarrow 17/2\ 9/2^-$
270.2±0.4	9±2	M1	12±3	$19/2\ 5/2^+ \rightarrow 17/2\ 5/2^+$
277.0±0.2	23±4	M1	30±5	$21/2\ 9/2^- \rightarrow 19/2\ 9/2^-$
285.8±0.1	69±10	E2	76±11	$17/2\ 1/2^- \rightarrow 13/2\ 1/2^-$
392.0±0.1	47±8	E2	49±8	$21/2\ 1/2^- \rightarrow 17/2\ 1/2^-$

(continued)

Table 1 (continued)

E_γ	Relative γ Intensity	Assigned Multi-polarity	Relative Transition Intensity	Transition Assignment
397.4±0.3	13±3	E2	14±3	$13/2\ 5/2^+ \rightarrow 9/2\ 5/2^+$
411.9±0.3	29±6	E2	30±6	$15/2\ 9/2^- \rightarrow 11/2\ 9/2^-$
448.2±0.2	18±3	E2	18±3	$15/2\ 5/2^+ \rightarrow 11/2\ 5/2^+$
459.2±0.3	14±3	E2	15±3	$17/2\ 9/2^- \rightarrow 13/2\ 9/2^-$
483.6±0.2	32±5	E2	33±5	$25/2\ 1/2^- \rightarrow 21/2\ 1/2^-$
489.5±0.2	15±3	E2	16±3	$17/2\ 5/2^+ \rightarrow 13/2\ 5/2^+$
499.0±0.3	22±4	E2	22±4	$19/2\ 9/2^- \rightarrow 15/2\ 9/2^-$
522.7±0.4	13±3	E2	13±3	$19/2\ 5/2^+ \rightarrow 15/2\ 5/2^+$
534.5±0.4	13±3	E2	13±3	$21/2\ 9/2^- \rightarrow 17/2\ 9/2^-$
559.4±0.3	25±5	E2	25±5	$29/2\ 1/2^- \rightarrow 25/2\ 1/2^-$

Table 2. Gamma-ray transitions observed in the $^{169}Tm(^{12}C,4n\gamma)^{177}Re$ reaction

E_γ	Relative γ Intensity	A_2	A_4	Assigned Multi-polarity	Relative Transition Intensity	Transition Assignment
84.7±0.1	80±25			E1	130±40	$5/2\ 5/2^+ \rightarrow 5/2\ 1/2^-$
122.3±0.2	42±4	0.036±.061	-0.056±.063	M1	168±16	$7/2\ 5/2^+ \rightarrow 5/2\ 5/2^+$
150.6±0.2	56±4	0.031±.029	-0.005±.029	M1	149±11	$9/2\ 5/2^+ \rightarrow 7/2\ 5/2^+$
163.5±0.1	100±4	0.097±.026	-0.025±.027	M1	229±10	$11/2\ 9/2^- \rightarrow 9/2\ 9/2^-$
176.3±0.2	52±5	0.106±.053	-0.159±.058	M1	107±11	$11/2\ 5/2^+ \rightarrow 9/2\ 5/2^+$
184.8±0.1	168±6	0.352±.024	-0.115±.026	E2	239±9	$13/2\ 1/2^- \rightarrow 9/2\ 1/2^-$
193.0±0.3	120±30	0.099±.017	-0.009±.019	M1	218±55	$13/2\ 9/2^- \rightarrow 11/2\ 9/2^-$
193.5±0.3	60±30			M1	109±55	$13/2\ 5/2^+ \rightarrow 11/2\ 5/2^+$
208.4±0.3	32±8			M1	51±13	$15/2\ 5/2^+ \rightarrow 13/2\ 5/2^+$
214.2±0.2	106±5	0.038±.040	0.060±.042	M1	171±8	$15/2\ 9/2^- \rightarrow 13/2\ 9/2^-$
235.6±0.2	67±5	0.052±.041	0.002±.044	M1	99±7	$17/2\ 9/2^- \rightarrow 15/2\ 9/2^-$
247.9±0.2	41±10			M1	58±14	$19/2\ 9/2^- \rightarrow 17/2\ 9/2^-$
304.6±0.1	154±7	0.367±.029	-0.124±.034	E2	168±8	$17/2\ 1/2^- \rightarrow 13/2\ 1/2^-$
326.9±0.3	27±5			E2	30±6	$11/2\ 5/2^+ \rightarrow 7/2\ 5/2^+$
356.5±0.3	12±3			E2	13±3	$13/2\ 9/2^- \rightarrow 9/2\ 9/2^-$
369.7±0.3	34±7			E2	36±7	$13/2\ 5/2^+ \rightarrow 9/2\ 5/2^+$

(continued)

Table 2 (continued)

E_γ	Relative γ Intensity	A_2	A_4	Assigned Multi-polarity	Relative Transition Intensity	Transition Assignment
402.9±0.3	31±4			E2	32±5	15/2 $5/2^+$ → 11/2 $5/2^+$
406.7±0.3	27±6			E2	28±6	15/2 $9/2^-$ → 11/2 $9/2^-$
413.7±0.1	117±7	0.233±.047	-0.048±.051	E2	121±7	21/2 $1/2^-$ → 17/2 $1/2^-$
449.9±0.2	47±5			E2	48±5	17/2 $9/2^-$ → 13/2 $9/2^-$
483.5±0.3	26±4			E2	27±4	19/2 $9/2^-$ → 15/2 $9/2^-$
509.7±1.0	120±50			E2	122±50	25/2 $1/2^-$ → 21/2 $1/2^-$
590.9±0.2	64±13	0.353±.059	-0.039±.063	E2	64±13	29/2 $1/2^-$ → 25/2 $1/2^-$
656.0±1.0	36±8			E2	36±8	33/2 $1/2^-$ → 29/2 $1/2^-$

Table 3. Mixing ratios for transitions in ^{177}Re obtained from the angular distribution data (col. 2) and the ratio of the cross-over and cascade transitions (col. 3).

Transition	Mixing Ratio (E2/M1) %	
	K = 5/2	
7/2 → 5/2	2.2 ± 1.4	–
9/2 → 7/2	3.2 ± 1.6	–
11/2 → 9/2	4.8 ± 3.9	1.8 ± 0.3
13/2 → 11/2	4.4 ± 2.7	1.2 ± 0.2
15/2 → 13/2	–	1.3 ± 0.5
	K = 9/2	
11/2 → 9/2	4.5 ± 1.6	–
13/2 → 11/2	4.4 ± 3.2	1.7 ± 0.3
15/2 → 13/2	2.9 ± 1.5	2.1 ± 0.4
17/2 → 15/2	3.1 ± 1.6	3.8 ± 0.7
19/2 → 17/2	–	2.3 ± 0.5

Table 4. Parameters obtained from the Coriolis coupling calculation for ^{181}Re, ^{179}Re, and ^{177}Re. The parameters A and a giving the best fit to ^{181}Re were used in fitting the other two isotopes.

Isotope	A (keV)	a	$B \times 10^3$ (keV)	Energy Separation 1/2[541], 3/2[532] (keV)
181	16.49	4.02	-5.71	355.
179	16.50†	4.0†	-7.41	652.
177	16.50†	4.0†	-6.06	1093.

†Fixed at ^{181}Re values.

Table 5. Comparison of experimental energy levels and those from the Coriolis coupling calculation for ^{177}Re. The squares of the amplitudes of the admixed wave functions are indicated.

J	E_{exp}	E_{calc}	Admixed wave function - (amplitude)^2				
			1/2[541]	3/2[532]	5/2[523]	7/2[514]	9/2[505]
1/2		-47.7	1.0(0)				
3/2		184.2	9.81(-1)	1.86(-2)			
5/2		-80.2	9.74(-1)	2.58(-2)	3.42(-4)		
7/2		432.2	8.82(-1)	1.11(-1)	7.3(-3)	3.99(-5)	
9/2	0.0	-2.8	9.37(-1)	6.01(-2)	2.67(-3)	2.14(-5)	2.18(-8)
11/2		729.1	6.99(-1)	2.55(-1)	4.57(-2)	9.52(-4)	2.81(-6)
13/2	184.8	188.2	8.97(-1)	9.5(-2)	7.36(-3)	1.30(-4)	4.49(-7)
17/2	489.4	491.4	8.57(-1)	1.28(-1)	1.41(-2)	3.99(-4)	2.49(-6)
21/2	903.1	901.6	8.18(-1)	1.58(-1)	2.24(-2)	8.84(-4)	8.24(-6)
25/2	1412.8	1410.2	7.80(-1)	1.86(-1)	3.21(-2)	1.63(-3)	2.05(-5)
29/2	2003.8	2005.3	7.42(-1)	2.12(-1)	4.28(-2)	2.69(-3)	4.30(-5)

Table 6. Comparison of experimental energy levels and those from the Coriolis coupling calculation for ^{179}Re. The squares of the amplitudes of the admixed wave functions are indicated.

J	E_{exp}	E_{calc}	Admixed wave function - (amplitude)^2				
			1/2[541]	3/2[532]	5/2[523]	7/2[514]	9/2[505]
1/2		-9.2	1.0(0)				
3/2		206.6	9.31(-1)	6.89(-2)			
5/2	< 0	-59.2	9.39(-1)	6.00(-2)	7.74(-4)		
7/2		386.0	6.79(-1)	3.04(-1)	1.68(-2)	8.57(-5)	
9/2	0	-1.5	8.79(-1)	1.16(-1)	4.92(-3)	3.84(-5)	3.87(-8)
11/2		608.8	4.77(-1)	4.62(-1)	6.01(-2)	1.10(-3)	3.00(-6)
13/2	168.7	170.8	8.26(-1)	1.62(-1)	1.17(-2)	2.00(-4)	6.76(-7)
17/2	454.5	455.5	7.81(-1)	1.98(-1)	2.02(-2)	5.51(-4)	3.35(-6)
21/2	846.5	845.4	7.40(-1)	2.29(-1)	2.99(-2)	1.13(-3)	1.02(-5)
25/2	1330.1	1328.7	7.02(-1)	2.55(-1)	4.06(-2)	1.98(-3)	2.41(-5)
29/2	1889.5	1890.3	6.65(-1)	2.80(-1)	5.24(-2)	3.13(-3)	4.85(-5)

UCRL-20494

Table 7. Comparison of experimental energy levels and those from the Coriolis coupling calculation for ^{181}Re. The squares of the amplitudes of the admixed wave functions are indicated.

J	E_{exp}	E_{calc}	Admixed wave function - (amplitude)^2				
			1/2[541]	3/2[532]	5/2[523]	7/2[514]	9/2[505]
1/2	432.0	432.0	1.00(0)				
3/2	600.0	600.0	7.00(-1)	3.00)-1)			
	867.0	867.0	3.00(-1)	7.00(-1)			
5/2	357	351.5	8.61(-1)	1.37(-1)	1.69(-3)		
9/2	387	386.5	7.89(-1)	2.03(-1)	8.02(-3)	6.03(-5)	5.92(-8)
13/2	542	542.8	7.40(-1)	2.43(-1)	1.62(-2)	2.64(-4)	8.64(-7)
17/2	818	817.4	7.04(-1)	2.71(-1)	2.51(-2)	6.48(-4)	3.80(-6)
21/2	1204	1204.1	6.72(-1)	2.92(-1)	3.44(-2)	1.22(-3)	1.06(-5)

FIGURE CAPTIONS

Fig. 1. Ge(Li) gamma-ray singles spectra following $^{172}Yb(^{11}B,4n)^{179}Re$ and $^{169}Tm(^{12}C,4n)^{177}Re$ reactions. Only transitions definitely assigned to ^{179}Re and ^{177}Re (and Coulomb excitation of the targets) are indicated.

Fig. 2. Excitation functions for some transitions in ^{179}Re, indicating the more rapid increase with energy associated with the higher angular momentum states.

Fig. 3. Excitation functions for some transitions in ^{177}Re, indicating the more rapid increase with energy associated with the higher angular momentum states.

Fig. 4. Spectra recorded in coincidence with the 185 keV and 214 keV transitions of ^{177}Re and the 169 keV and 218 keV transition of ^{179}Re. Coincidences with the background under each transition have been subtracted. Random coincidences are not significant and no corrections for these have been made.

Fig. 5. Partial level scheme for ^{179}Re. The relative position of the 9/2 $9/2^-[514]$ and 5/2 $5/2^+[402]$ states has not been determined. The rotational transition 9/2 $1/2^- \rightarrow$ 5/2 $1/2^-$ has not been observed in this work, the 57.7 keV indicated is predicted by the Coriolis coupling calculation. Transition intensities are shown in parentheses.

Fig. 6. Partial level scheme for ^{177}Re. The relative position of the 9/2 $9/2^-[514]$ and 5/2 $1/2^-[541]$ states has not been determined. The rotational transition 9/2 $1/2^- \rightarrow$ 5/2 $1/2^-$ has not been observed in this work, the 77.5 keV indicated is predicted by the Coriolis coupling calculation. Transition intensities are shown in parentheses.

Fig. 7. Energy of the lowest observed rotational transition based on the $1/2^-[541]$, $9/2^-[514]$, and $5/2^+[402]$ states plotted as a function of neutron number. The $2^+ \rightarrow 0^+$ transitions of the neighbouring doubly-even W and Os isotopes are shown for comparison.

Fig. 8 a) Excitation energy (above 5/2 $5/2^+[402]$) of some states observed in the odd-A rhenium isotopes. Extrapolation to lower mass (dotted lines) indicates that the states 5/2 $5/2^+[402]$, 9/2 $9/2^-[514]$, and 9/2 $1/2^-[541]$ should lie very close to each other in ^{179}Re and ^{177}Re.

b) Relative populations of the rotational bands observed in heavy ion, xn reactions (expressed as a percentage of the total population of these bands) as a function of mass number. The variation is consistent with the extrapolation of fig. 8a.

Fig. 9. Single-particle energies as a function of the hexadecapole moment ϵ_4, for a fixed quadrupole deformation $\epsilon = 0.25$. See Ref. [28]).

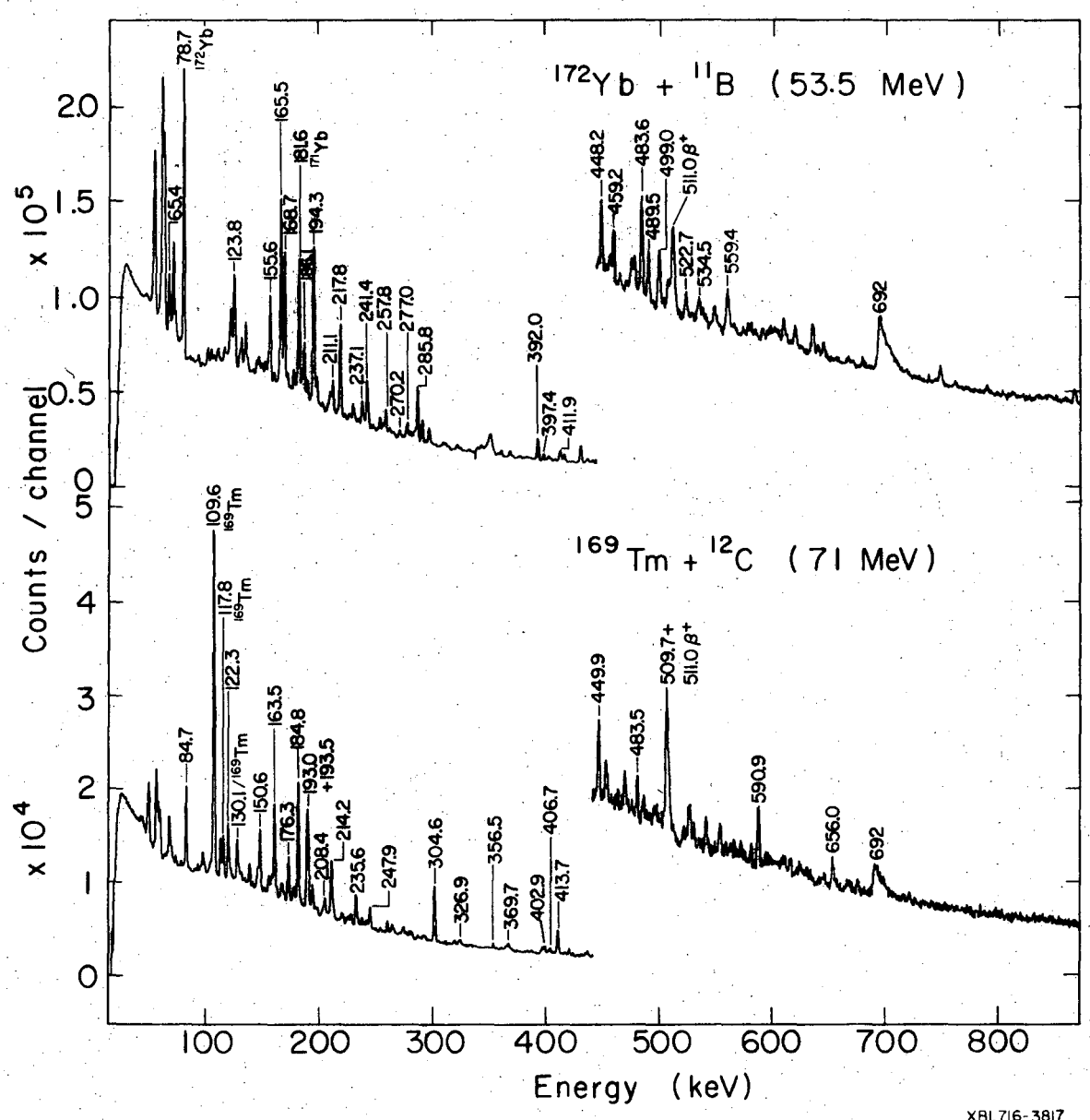
^{172}Yb + ^{11}B (53.5 MeV)
^{169}Tm + ^{12}C (71 MeV)
Counts / channel
x 10^5
x 10^4
Energy (keV)
78.7 ^{172}Yb
165.5
181.6 ^{171}Yb
123.8
155.6
168.7
194.3
217.8
241.4
257.8
277.0
211.1
237.1
270.2
285.8
392.0
397.4
411.9
448.2
459.2
483.6
489.5
499.0
511.0 β$^+$
522.7
534.5
559.4
692
109.6 ^{169}Tm
117.8 ^{169}Tm
122.3
84.7
130.1 / ^{169}Tm
150.6
163.5
176.3
184.8
193.0
+193.5
208.4
214.2
235.6
247.9
304.6
326.9
356.5
369.7
402.9
406.7
413.7
449.9
483.5
509.7+
511.0 β$^+$
590.9
656.0
692
XBL716-3817

Fig. 1

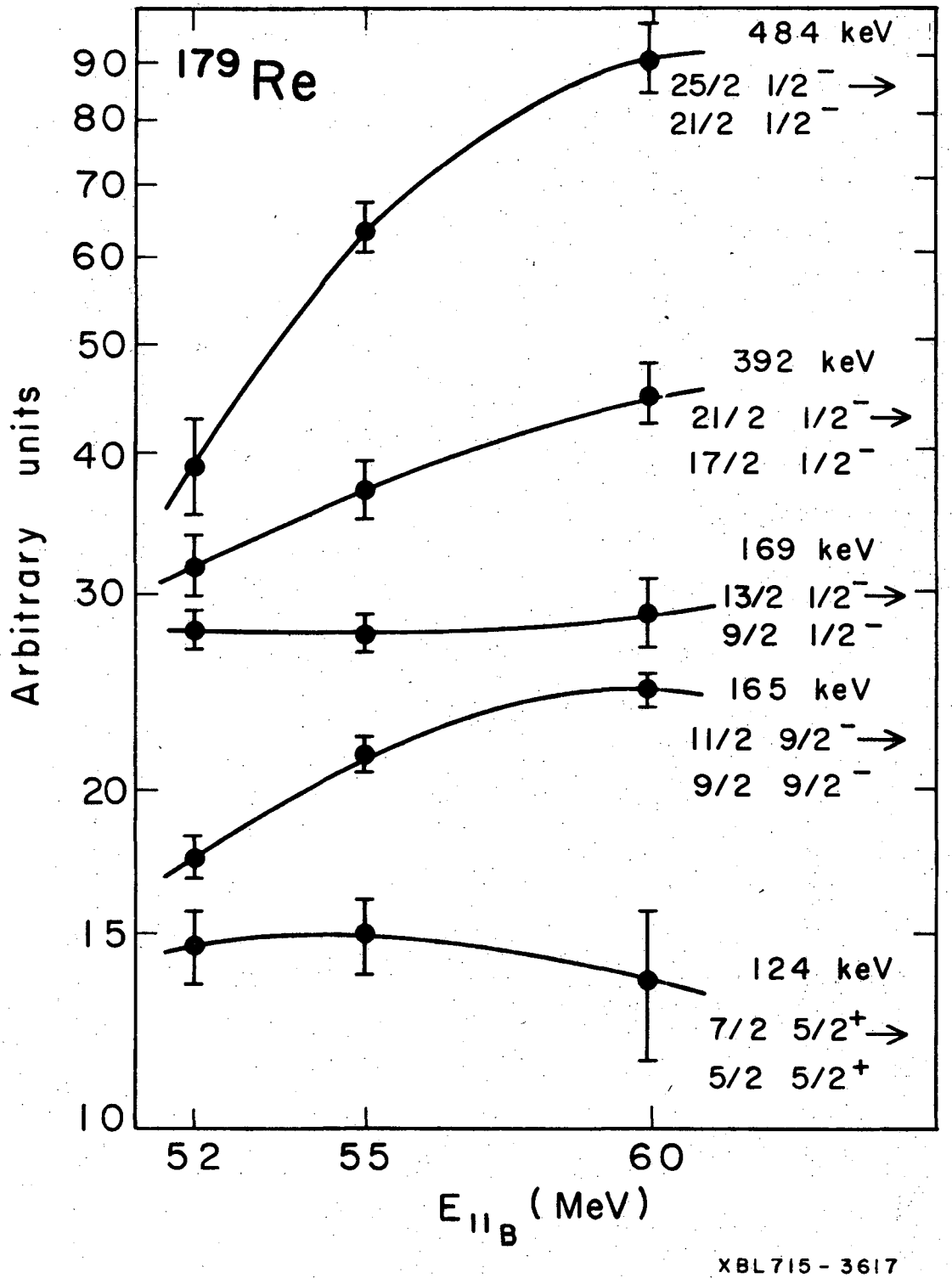
179 Re
484 keV
25/2 1/2⁻ →
21/2 1/2⁻
392 keV
21/2 1/2⁻ →
17/2 1/2⁻
169 keV
13/2 1/2⁻ →
9/2 1/2⁻
165 keV
11/2 9/2⁻ →
9/2 9/2⁻
124 keV
7/2 5/2⁺ →
5/2 5/2⁺
Arbitrary units
90
80
70
60
50
40
30
20
15
10
52
55
60
E11B (MeV)
XBL715-3617

Fig. 2

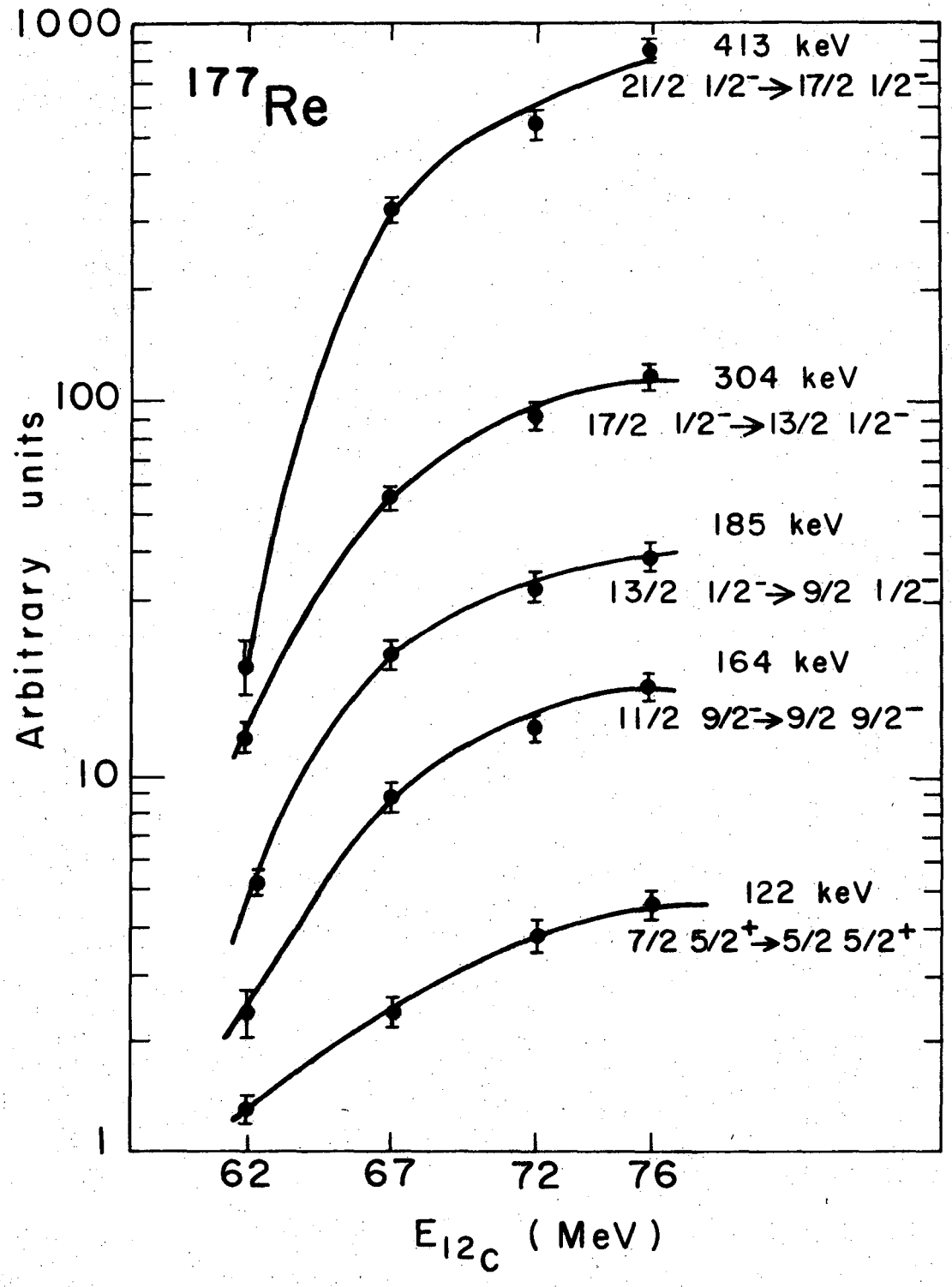

XBL715-3616

Fig. 3

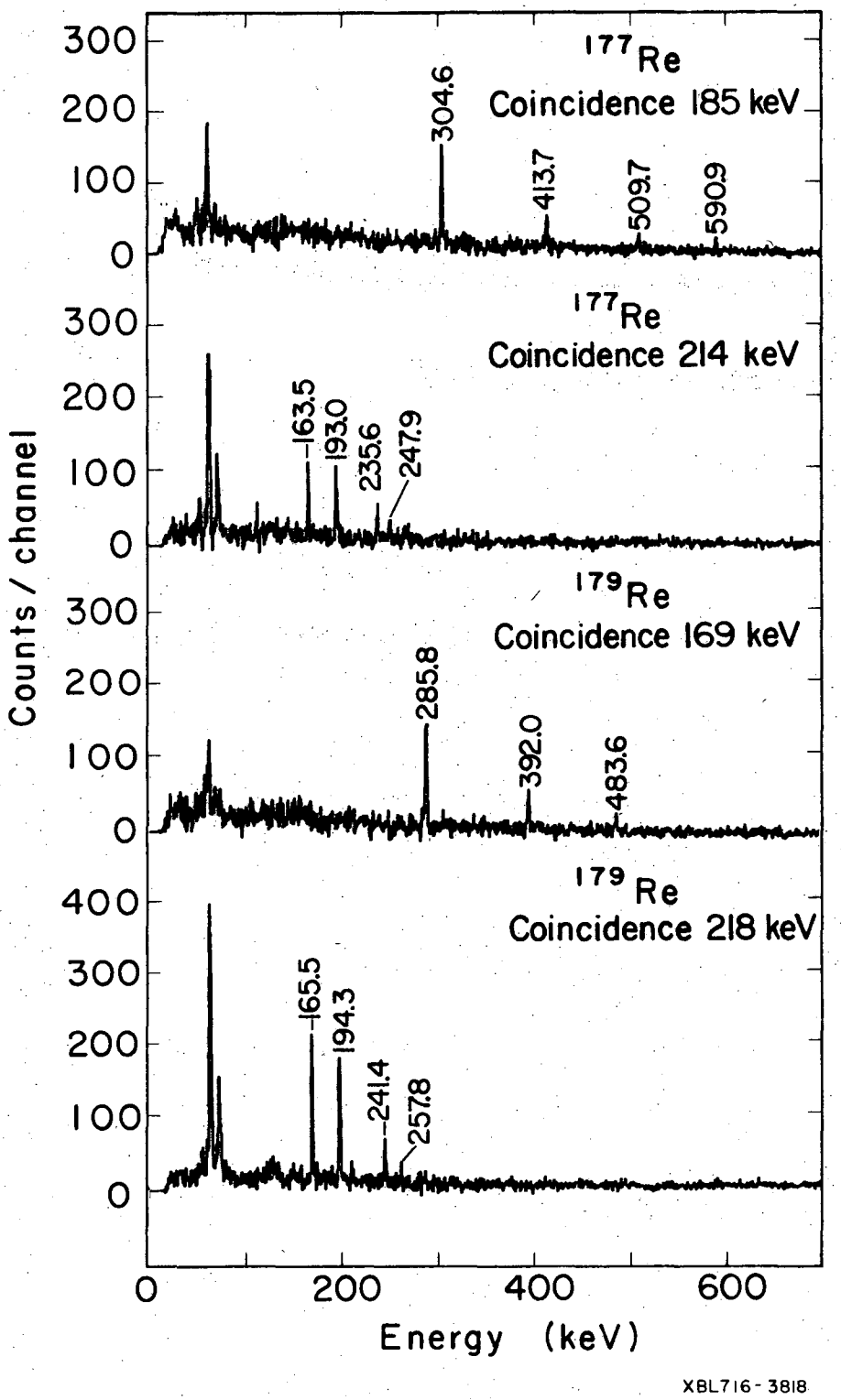
177Re
Coincidence 185 keV
304.6
413.7
509.7
590.9
177Re
Coincidence 214 keV
163.5
193.0
235.6
247.9
179Re
Coincidence 169 keV
285.8
392.0
483.6
179Re
Coincidence 218 keV
165.5
194.3
241.4
257.8
Counts / channel
Energy (keV)
XBL716-3818

Fig. 4

Rotational bands of ^{179}Re

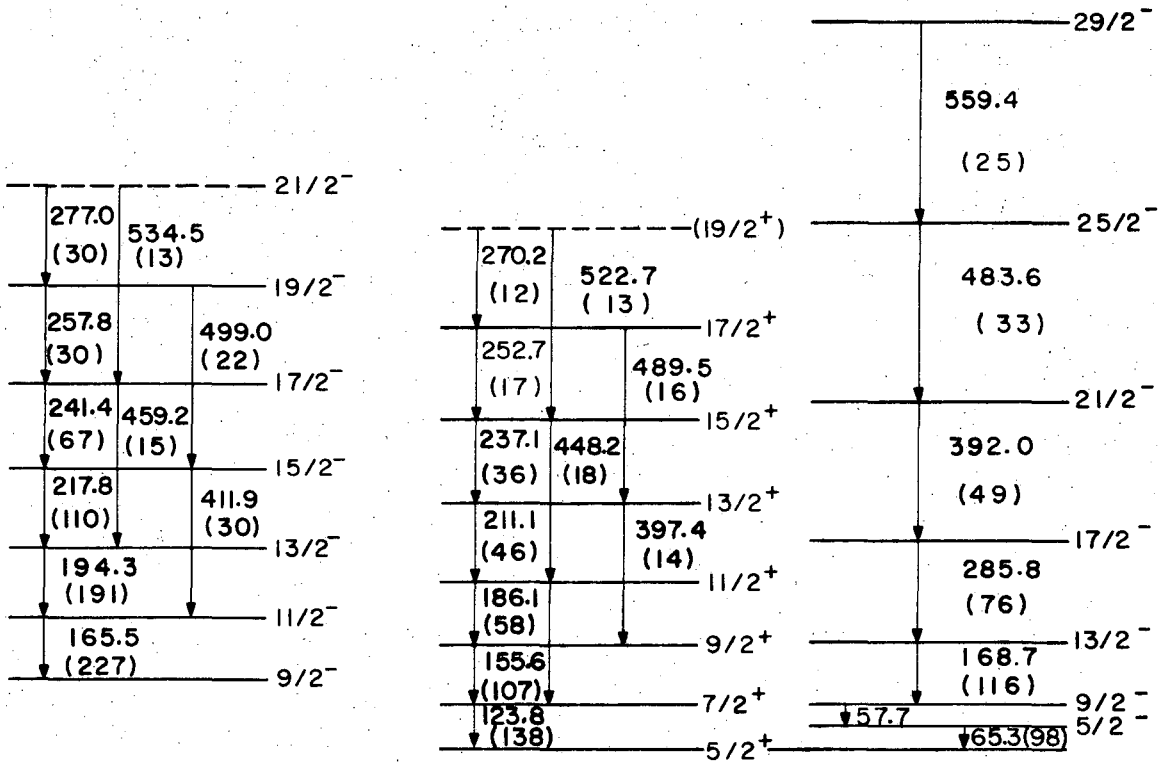

XBL715-3612

Fig. 5

Rotational bands of ^{177}Re

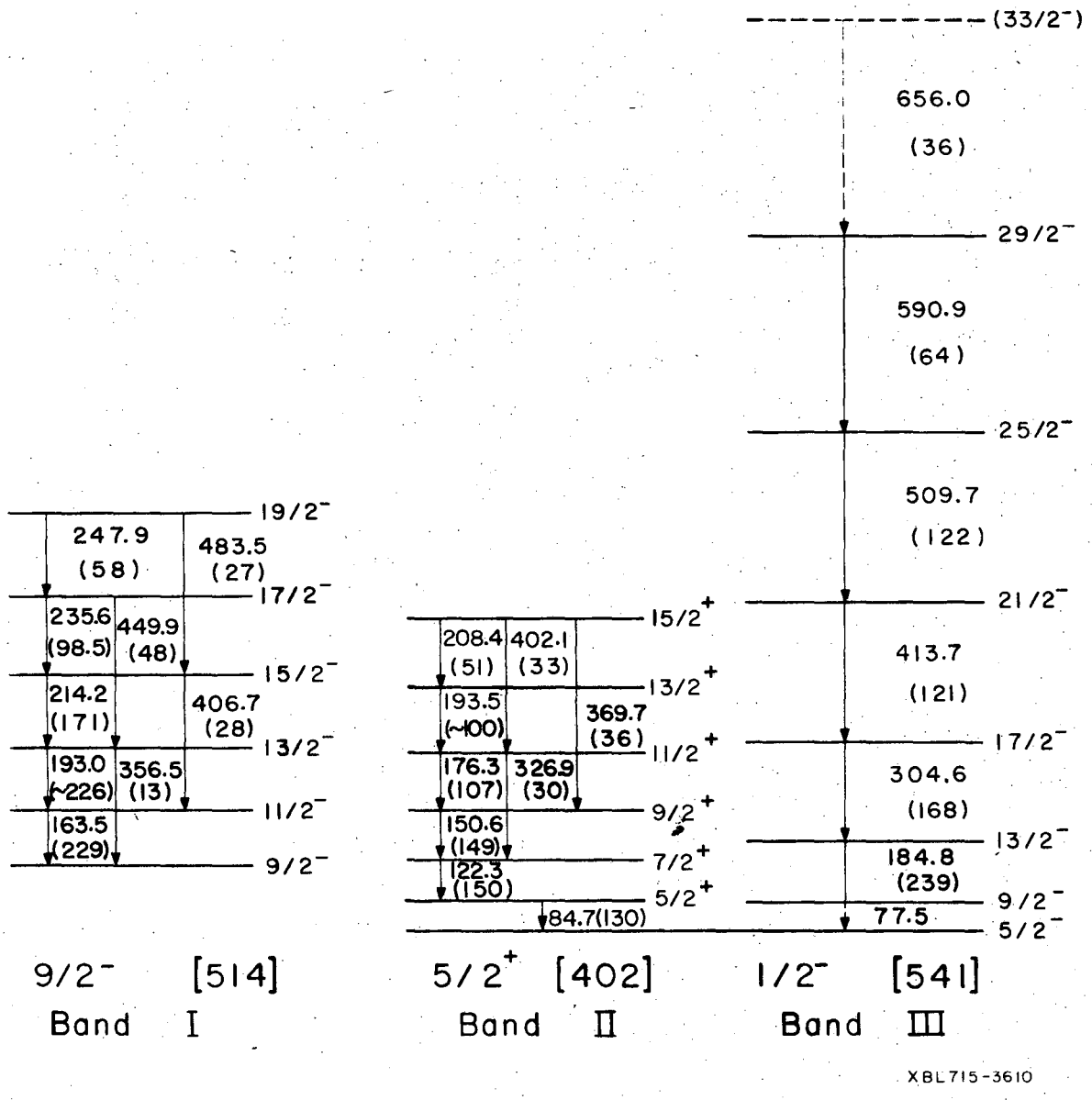

Fig. 6

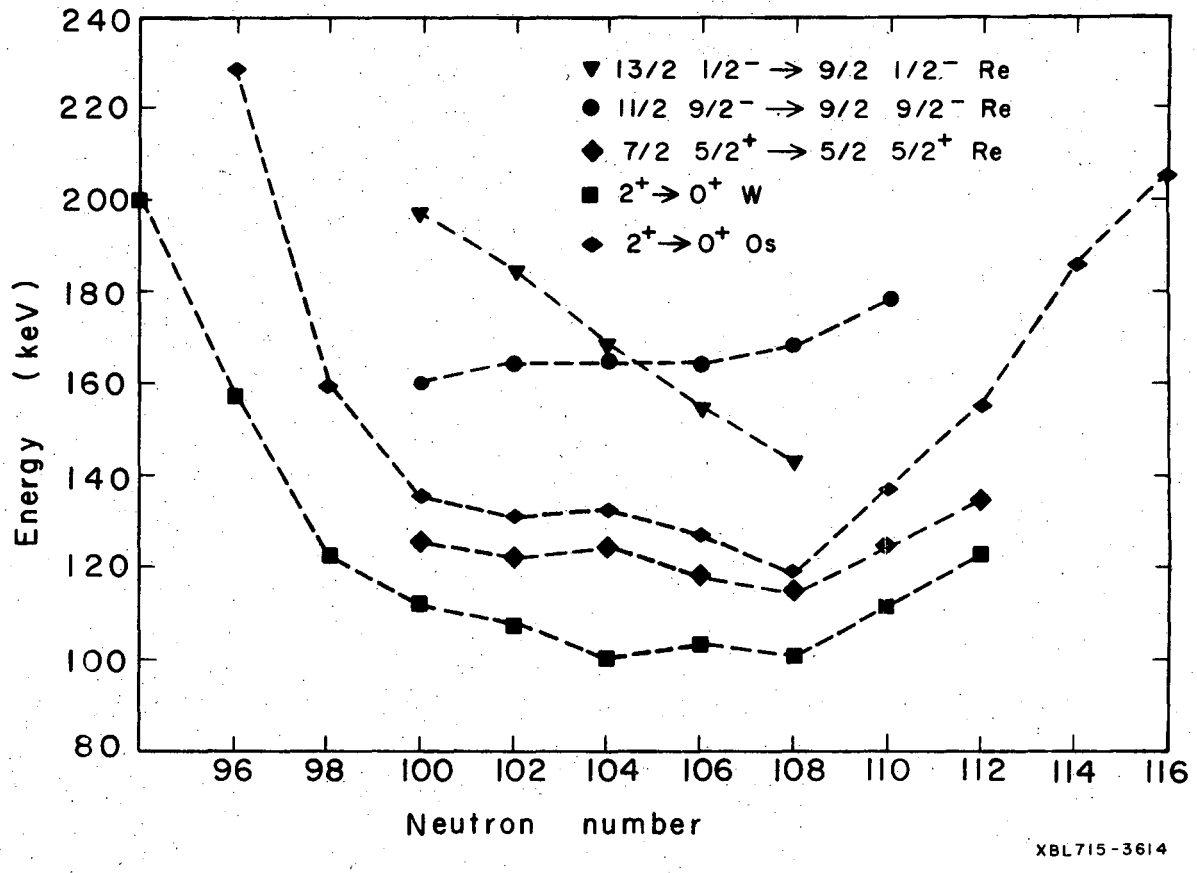
13/2 1/2⁻ → 9/2 1/2⁻ Re
11/2 9/2⁻ → 9/2 9/2⁻ Re
7/2 5/2⁺ → 5/2 5/2⁺ Re
2⁺→ 0⁺ W
2⁺→ 0⁺ Os
Energy (keV)
240
220
200
180
160
140
120
100
80
96
98
100
102
104
106
108
110
112
114
116
Neutron number
XBL715-3614

Fig. 7

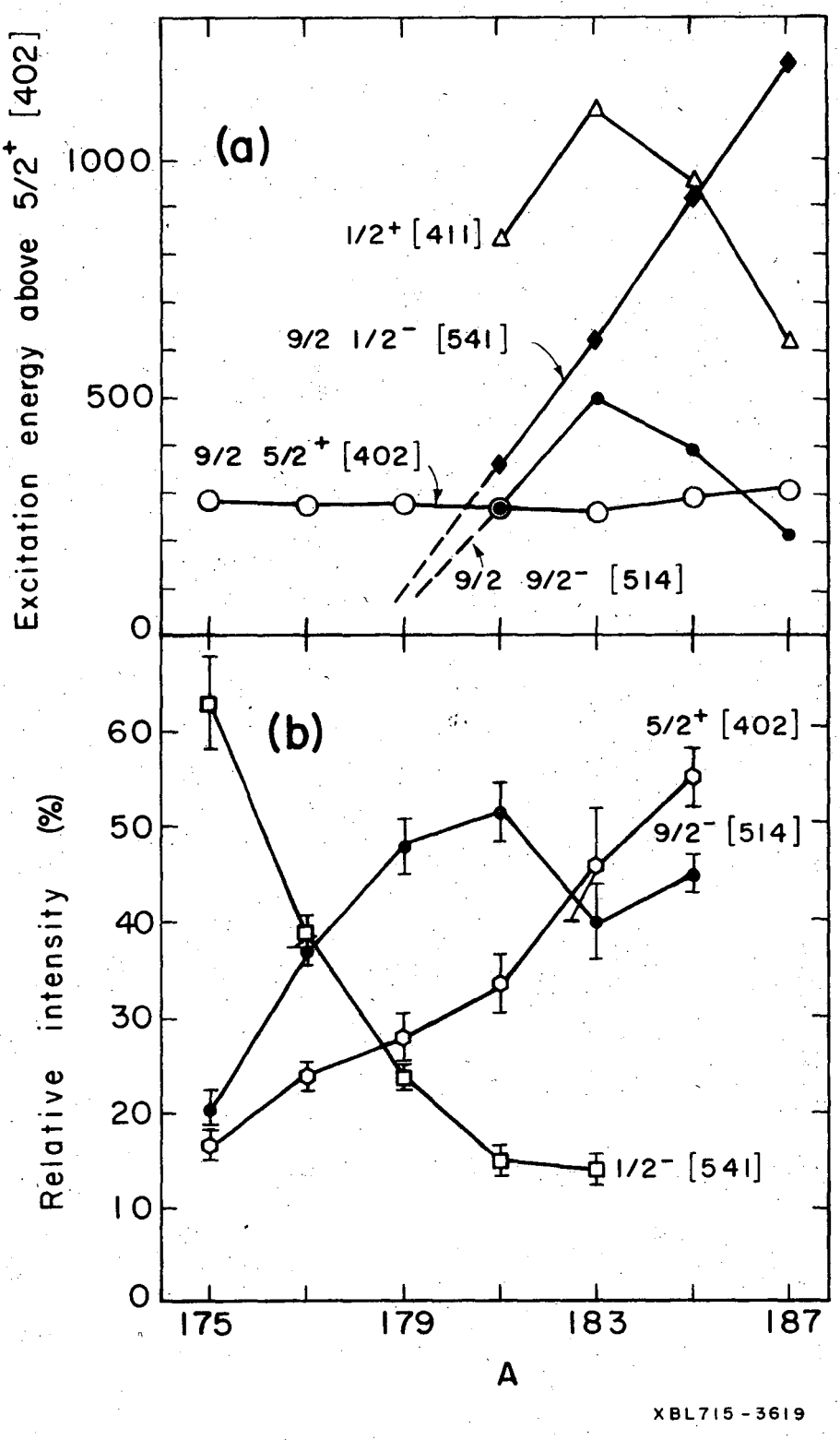
(a)
Excitation energy above 5/2+ [402]
1000
500
0
1/2+ [411]
9/2 1/2- [541]
9/2 5/2+ [402]
9/2 9/2- [514]
(b)
Relative intensity (%)
60
50
40
30
20
10
0
5/2+ [402]
9/2- [514]
1/2- [541]
175
179
183
187
A
XBL715-3619

Fig. 8

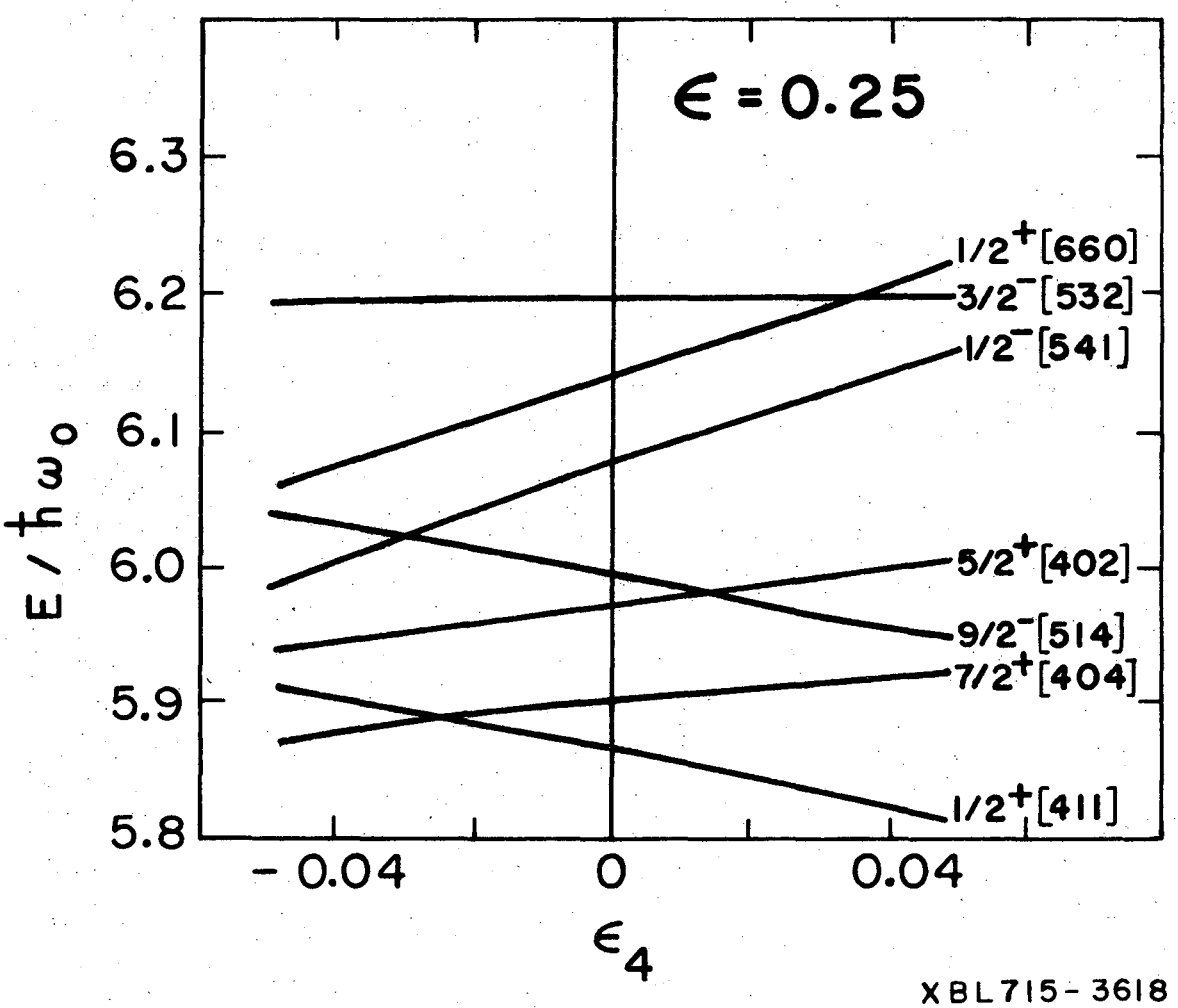
ϵ = 0.25
6.3
6.2
6.1
6.0
5.9
5.8
E / ħω₀
- 0.04
0
0.04
ϵ₄
1/2⁺[660]
3/2⁻[532]
1/2⁻[541]
5/2⁺[402]
9/2⁻[514]
7/2⁺[404]
1/2⁺[411]
XBL715-3618

Fig. 9

TECHNICAL INFORMATION DIVISION
LAWRENCE BERKELEY LABORATORY
UNIVERSITY OF CALIFORNIA
BERKELEY, CALIFORNIA 94720